Effects of Interface Roughness on Shear Key Performance of Ultra-High Performance Concrete in Adjacent Box Girder Bridges

Husam H. Hussein [a], Fouad T. Al Rikabi [b], and Shad M. Sargand [c]

(a) Ph.D., Research Scholar, Civil Engineering, Ohio University, Athens, OH, USA. ORCID: https://orcid.org/0000-0002-4657-2499. Email:husam.hussein@outlook.com; h236310@ohio.edu
(b) Ph.D., Candidate, Civil Engineering, Ohio University, Athens, OH, USA. ORCID: https://orcid.org/0000-0002-4150-4622. Email:fouad.alrikabi@outlook.com; fs018011@ohio.edu
(c) Ph.D., Russ Professor, Civil Engineering, Ohio University, Athens, OH, USA

Abstract:

For decades, adjacent box girder bridges have shown good performance and service life. However, longitudinal joints connecting the adjacent box girders may be susceptible to a degradation, including cracking and debonding, under a large number of load and thermal cycles. Although ultra-high-performance concrete (UHPC) has been used for joints in the highway bridges to eliminate the longitudinal cracks in shear keys, there is limited information regarding the effect of bond strength between UHPC and high strength concrete (HSC) on the load transfer mechanism in the transverse direction between adjacent box girders. The aim of this study is to use experimental results and finite element (FE) analysis of direct shear tests to evaluate the performance of optimized shape of the UHPC shear key (OPT-UHPC). The FE models, along with three types of shear key roughness, were calibrated and validated with previously published laboratory experimental results by the authors. Three types of interface roughness (smooth, mid-rough, and rough) between UHPC and HSC components were employed to investigate the load transfer mechanism between concrete components. The results of numerical simulations of OPT-UHPC joint model using interface models with different roughness types were compared, the results of the analysis show that joint with a smooth surface is sufficient for load transfer between HSC components, and that joint with a mid-rough surface is capable of transferring load up to failure in the HSC components. The results can be used as a guidance when designing connection between adjacent box beams in bridges.

Keywords: Ultra-high-performance concrete; UHPC; High strength concrete; HSC; Interfacial properties; Bridge connections; Finite element method; Shape optimization; interface bond**.**

1 Introduction

For decades, adjacent box girder bridges have shown good performance and service life (Russell 2009; Aktan et al. 2005; Lall et al. 1998; Miller et al. 1999; El-Remaily et al. 1996). However, longitudinal joints connected the adjacent box girders may be susceptible to a frequent degradation, including cracking and debonding, under a large number of load and thermal cycles. The joint cracking and debonding allow corrosive agents through and saturate the girder sides, thus accelerating deterioration of the bridge. In order to improve shear key strength and durability, past research recommends use of a new grout material having superior mechanical properties such as high bond and tensile strengths. Recently, ultra-high-performance concrete (UHPC) material has been proposed by Federal Highway Administration (FHWA) as a grout material to fill connections between adjacent girders (Graybeal, 2014). UHPC has received attention from engineers and researchers to be used in a variety of applications for improving the performance of highway bridges. Unlike regular grout, UHPC has superior properties such as increased strength, long-term stability, and exceptional durability (Graybeal, 2006). Also, the material exhibits increased adhesive strength for different types of surface roughness compared to normal grout material (Hussein et al., 2016). Several highway bridges have been constructed using UHPC as grout material, and summaries of these can be found in the literature (Russell and Graybeal, 2013; Graybeal, 2014).

Past research has investigated three main parameters – the grout material, different levels of transverse post-tensioning (TPT) stress, and the shear key configuration – with the aim of enhancing the shear key performance of adjacent box girder bridges. The performance of typical shear keys has been evaluated in terms of bond strength, ultimate strength capacity, and mode of failure, as measured in tests of direct shear, flexural, and direct tension (Gulyas et al., 1995; Gulyas and Champa, 1997; Issa et al., 2003; Porter et al., 2011). On the other hand, several studies have investigated load transfer mechanisms between the adjacent box girders through the typical shear key configuration along with TPT ties either by testing a full-scale bridge or a partial bridge structure (El-Remaily et al., 1996; Grace, et al., 2012; Hussein, et al., 2017b; Miller, et al., 1999; Yuan and Graybeal, 2016). However, these studies provided only limited information on the failure mode of the shear keys and on the strains experienced during applied loads. Also, DOTs and standard codes do not provide any information regarding the design of the shear key configuration (Russel 2009 and 2011). Selection of the connection type depends on the use or absence of TPT ties as well as the type and stress level of TPT ties. Also, it depends on the use or absence of shear reinforcement bars and the type of grout material. Many researchers have reported that using a grout material having high bond strength can improve the load transfer mechanism between concrete components (Gulyas and Champa, 1997; Gulyas et al., 1995; Issa et al., 2003; Miller et al., 1999). Others reported that changing shear key configuration may increase the ultimate load capacity and enhance the load transfer mechanism. The most recent type of grout material used in shear key connections is UHPC material, and this material enhances the overall performance of the bridge superstructure. Although UHPC has been used for joints in the highway bridges to eliminate the longitudinal cracks in shear keys, there is limited information regarding the effect of bond strength between UHPC and high strength concrete (HSC)on the load transfer mechanism in the longitudinal direction between adjacent box girders.

Research to date on UHPC for connection elements in bridges indicates an improvement in the performance of the overall bridge superstructure. The improvement in performance can be attributed to the higher strength of the UHPC relative to traditional grouting materials and the

higher bond strength between the UHPC and other bridge components due to the high adhesion of the UHPC material (Hussein et al., 2016). While the significance of adhesion on the bond strength of UHPC has been demonstrated in laboratory test specimens, there is limited information on the effect of these properties of the UHPC on the load transfer mechanism between adjacent box-beams. An economical approach to analyzing the UHPC joint is through finite element (FE) modeling. In a recent study by Hussein et al. (2018a), three 3D finite element models simulating direct shear, flexural, and direct tension tests were utilized to develop and design a new UHPC shear key. These models were calibrated and validated with experimental data reported by Hussein et al. (2017a). Hussein et al. (2018a) compared these models with different shear key configurations from past research and existing design standards to study the effects of the shear key configuration on the load transfer mechanism. The researchers optimized the shape of the UHPC shear key in attempt to enhance load transfer mechanism and increase the ultimate strength capacity. Finally, Hussein et al., (2018b) experimentally investigated the performance and ultimate load capacity of the OPT-UHPC shear key between two HSC components using direct shear, direct tension, and flexural tests.

2 Objectives

The aim of this study is to use experimental results and finite element (FE) analysis of direct shear tests to evaluate the performance of the optimized UHPC (OPT-UHPC) and FHWA-UHPC shear keys. The FE models, along with three types of shear key roughness, were calibrated and validated with previously published laboratory experimental results by the authors. Three types of interface roughness (smooth, mid-rough, and rough) between UHPC and high strength concrete (HSC) components were employed to investigate the load transfer mechanism between concrete components of OPT-UHPC and FHWA-UHPC shear keys.

3 Finite Element Models

Two different three-dimensional FE models of the OPT-UHPC and FHWA-UPHC shear key configurations were developed to investigate the load transfer mechanism under direct shear load. These models were calibrated and validated using experimental data from the previous study by Hussein et al. (2017a and 2018b). The same models along with different types of interface roughness were used to study the effects of the shear key configuration and the interface roughness on the load transfer mechanism.

3.1 Experimental Program

The direct shear tests were based on load test configurations used and described in Hussein et al., (2017a and 2018b). The FHWA-UHPC and OPT-UHPC shear key shapes used for the test specimens are shown in Figure 1(a) and Figure 1(b), respectively. The FHWA-UHPC shear key was designed by Graybeal (2014), and the OPT-UHPC was designed by Hussein et al. (2017a and 2018b). Test specimens were constructed by connecting two HSC components with a UHPC shear key, as shown in Figure 1(b) (Hussein et al., 2017a) and Figure 1(d) (Hussein et al., 2018b).

The average compressive strength of the UHPC grout was 158.5±8 MPa (22.99±1.16 ksi) for all specimens. For HSC material, the compressive, flexural, and splitting tensile strengths at time of testing were 75, 5.3, and 4.8 MPa (10.8, 0.77, and 0.70 ksi), respectively for all specimens. A rough surface with exposed aggregate was adopted for the shear key surfaces. Also, the rough surface was recommended for joints in section 5.14.1.3.2 of the AASHTO LRFD (2012) and for UHPC joints by Graybeal (2014) and Hussein et al. (2016). Three specimens of each shear key configuration (see Figure 1(b and d)) were tested to obtain the maximum shear capacity of the

UHPC joint, and the specimens were 127 mm (5 in) deep (Hussein et al., 2017a, 2018b). A special steel frame was installed around the top and bottom concrete parts to prevent concrete failure at the specimen flanges or any lateral failure, as shown in Figure 1(b and d). The load and deflection were recorded until the specimen failed. More detailed information on these tests can be found in Hussein et al. (2017a and 2018b).

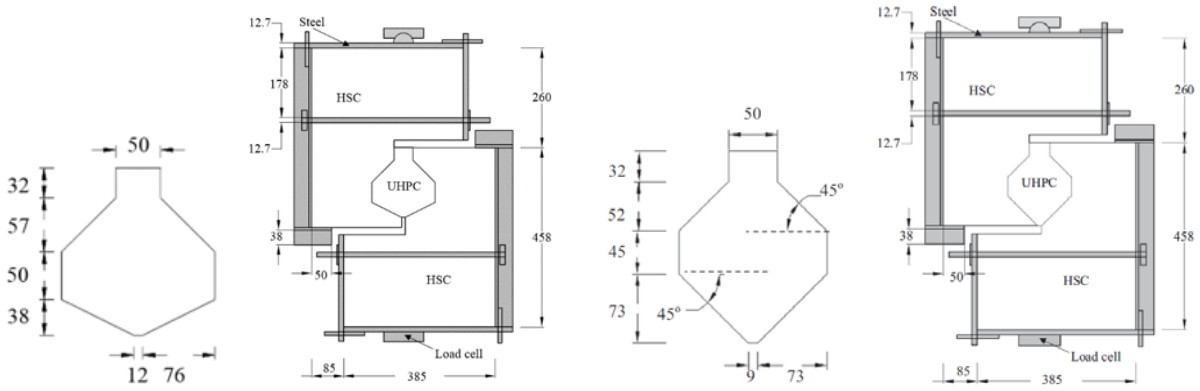

(a) (b) (c) (d)

Figure 1. (a) FHWA-Shear key dimensions; (b) direct shear specimen; (c) OPT-Shear key dimensions; (d) direct shear specimen. (Note: 1 cm = 0.39 in, 1 N =0.22 lb)

3.2 Finite Element Modeling

In this study, all FE analyses were accomplished using the commercial software package *ABAQUS*. FE model representing the direct shear test was calibrated and validated using the experimental testing data to study the FHWA-UHPC and OPT-UHPC shear key performances. The FE model of the direct shear test consisted of five components: UHPC shear key, two HSC parts, two steel frames, support, and loading cylinder, as shown in Figure. 2(a-c). Boundary conditions were applied to the bottom of the steel cylinder to restrain its vertical and horizontal movement, and the load was applied to the top cylinder, as shown in Figure. 2(a and e). In order to capture the behavior of the direct shear specimen with the steel frame at each side of the specimen, the steel frame was modeled in the FE program, as shown in Figure. 2(c).

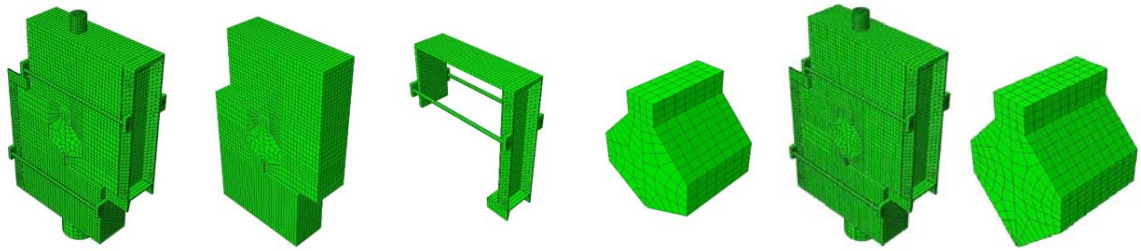

(a) (b) (c) (d) (e) (f)

Figure. 2. (a) FHWA-direct shear test; (b) HSC and UHPC parts; (c) steel frame; (d) FHWA-shear key (e) OPT-direct shear test: and (f) OPT-shear key

A friction coefficient of 1.0 and hard contact were used to simulate the tangential and normal behaviors at the interface between the steel frame and the HSC components. In order to produce a uniform element shape for obtaining better results when using *ABAQUS*, several partitions were formed throughout the models. Also, a higher density mesh was used at interface between UHPC-HSC contact areas in order to enhance the interface behavior, as shown in Figure.

2(d and f). The steel, UHPC, and the HSC components were modeled with 8-node brick elements, with a maximum mesh size of 10 mm (0.4 in.). Model calibration and validation were achieved by loading the UHPC-HSC specimens to failure, and comparing the results with the experimental test data.

3.3 Material and Interface Models

The concrete damage plasticity (CDP) and traction-separation constitutive models were employed to simulate concrete constitutive behaviors of UHPC and HSC materials and the interface behavior between UHPC and HSC components, respectively. The CDP model was used to model the nonlinear behavior of UHPC and HSC materials due to its ability to represent the concrete tension and compression responses. To define the elastic behavior of the UHPC and HSC, the modulus of elasticity and Poisson's ratio were specified from experimental tests on material specimens using ASTM protocols (see Table 1). Also, the CDP model in ABAQUS utilizes several specific material parameters, including tension stiffening and compression softening of the UHPC and HSC. A softening stress-strain relationship was used to represent strain softening beyond the ultimate compressive strength. Additionally, the CDP model requires additional parameters, which are listed in Table 1. For the steel components, Young's Modulus of a 207 GPa (30000 ksi) and Poisson's Ratios of 0.3 were used to define the elastic properties of steel.

Table 1. UHPC and HSC Properties used in FE Modeling

Property	UHPC	HSC
Modulus of elasticity GPa	53 [c]	41 [c]
Poisson's ratio	0.19 [c]	0.17 [c]
Compressive strength MPa	158.58 [c]	75 [c]
Maximum tensile stress MPa	15.9[a]	4.8[c]
Fracture energy G_f N/m	87,559[a]	120[b]
Dilation angle ψ	15[o a]	36[o b]
Eccentricity ϵ	0.1 [a]	0.1 [b]
σ_{b0}/σ_{c0}	1.16 [a]	1.16 [b]
K_c	2/3 [a]	2/3 [b]
Viscosity parameter μ	0.0 [a]	0.001[b]

[a] Chen and Graybeal (2010, 2011a, 2011b), [b] ABAQUS, [c] test by Hussein (2017c)

(Note: 1 cm = 0.39 in, 1 N =0.22 lb, 1 ksi = 6.89 MPa)

Also, the traction-separation constitutive model considers friction and adhesion at the interface between the UHPC and HSC materials. The traction-separation behaviors are linear elastic traction-separation, damage initiation criteria, and damage evolution models. Normal stiffness (K_n) and tangential stiffness (K_s and K_r) components for the linear elastic traction-separation model are the normal and tangential stiffness components that relate to the normal and shear separation across the interface before the initiation of damage. The damage at the interface occurs when the following quadratic stress-based damage interface criterion (DIC) for a cohesive surface is satisfied. The mechanical properties of the rough, mid-rough, and smooth interfaces are listed in Table 2 (Hussein et al., 2017c; Sargand et al., 2017). In addition to using the traction-separation constitutive model, normal and tangential behaviors at the UHPC shear key and HSC component interfaces were modelled using hard contact and friction, respectively.

Table 2. Mechanical Properties of Interface

Properties	Smooth	Mid-rough	Rough
Knn (N/mm^3)	1,358	1,358	1,358
Kss and Ktt (N/mm^3)	20,358	20,358	20,358
t_n^o, t_s^o, and t_t^o (Mpa)	3.02	5.01	5.63
Total/Plastic displacement (mm)	0.018	0.117	0.241
Stabilization	0.001	0.001	0.001

(Note: 1 cm = 0.39 in, 1 N =0.22 lb, 1 ksi = 6.89 MPa)

4 Results and Discussion

4.1 Model Calibration

The simulation of interfaces between the UHPC and HSC in the previous work by the authors (Hussein et al., 2017c; Sargand et al., 2017) demonstrated that the interface parameters and friction coefficients for the rough surface roughness can be used to simulate the interface behavior in UHPC-HSC connections. The validated rough interface model was used to simulate the behavior of two HSC components connected by a UHPC joint. However, calibration of the fracture energy of CDP model was first necessary in order to identify the tension stiffening of the HSC components. The model calibration gave a fracture energy of 108 N/m, and the agreement between the simulated and experimental vertical deflections is shown in Figure 3. In this figure, good agreement between the simulated and experimental results for the model was obtained.

For OPT-UHPC shear key model, the same CDP and rough interface parameters of the FHWA-UHPC shear key model were used. Comparisons of the experimental deflections with FE results for the FHWA-UHPC and OPT-UHPC configurations are shown in Figure 3(a) and Figure 3(b), respectively. As can be seen, OPT-UHPC joint exhibited large deflection with high load capacity compared to the FHWA-UHPC joint. Moreover, the OPT-UHPC shear key configuration enhanced the maximum load capacity with the same maximum principle and shear strain values compared to the FHWA-UHPC shear key configuration, as presented in Figure 4. The OPT-UHPC shape has a better stress distribution between the concrete components via UHPC shear key.

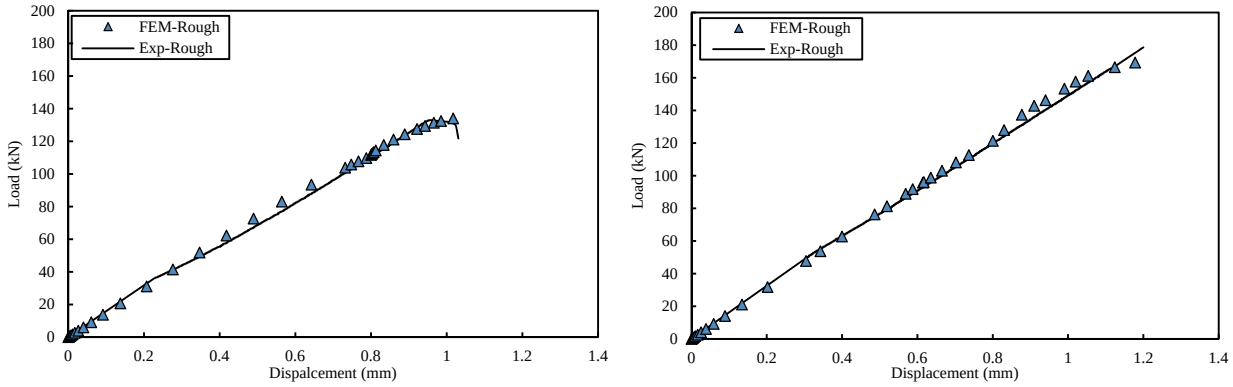

Figure 3. Load-displacement plot of direct shear specimen using (a) FHWA-UHPC shear key configuration and (b) OPT-UHPC shear key configuration (Note: 1 cm = 0.39 in, 1 N =0.22 lb)

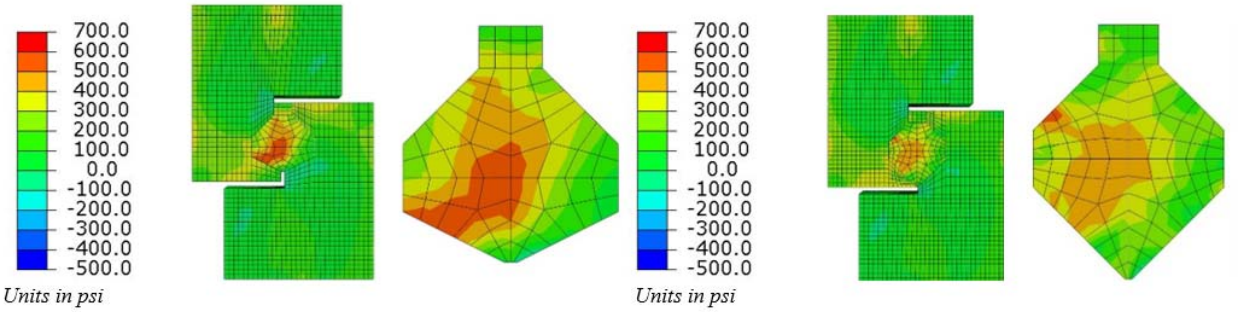

(a) (b)

Figure 4. Maximum principal stress distribution at 92 kN (20.68 kip) load: (a) Type IV shape; (b) Type OPT shape.

4.2 UHPC-HSC Interface Roughness Comparison

The strong bond at the UHPC-HSC interface can be attributed, in part, to the high adhesion of the UHPC combined with the increased bonding surface due to the exposed aggregate on the HSC. While this leads to an effective load transfer mechanism between HSC components, achieving the exposed aggregate surface requires a special preparation. An improvement in constructability and a reduction in cost could be achieved by using a connection that requires less surface preparation, i.e. the untreated (smooth) or sandblasted (mid-rough) surfaces, and an investigation into the effect of these surface roughness types on the joint performance is warranted. Therefore, additional simulations were conducted for the FHWA-UHPC shear key model where the values for the interface parameters were selected to be consistent with the smooth, mid-rough, and rough surfaces. The models were loaded until the failure took place for all three surface roughness types. A comparison of the deflections for the different surface roughness types is shown in Figure 5. Figure 5(a) demonstrates that the deflections of FHWA-UHPC shear key are different, and the surface roughness has effect on the global shear key behavior for the loading case considered. However, there is small difference in the ultimate capacity between rough and mid-rough models while there is a large difference between the smooth and other roughness types. That is to say, the UHPC-HSC connections with the rough and mid-rough surfaces remain fully bonded, and are almost equally effective in transferring the load between concrete components. For the smooth model, the de-bonding between UHPC and HSC was accorded at load of 87.5 kN (19.7 kip). The result once again demonstrates the contribution of the adhesion to the bond strength at the interface, and suggest that sufficient load transfer could be achieved for UHPC-HSC connections with untreated surfaces, resulting in improved constructability and a reduction in cost.

For the OPT-UHPC shear key model, the OPT-UHPC shear key design was studied by modeling direct shear specimens using the same material properties and interface surface roughness. Figure 5(b) shows that the deflections of OPT-UHPC shear key are different, and the surface roughness has significant effect on the global shear key behavior. There is a large difference between rough and mid-rough models, and the same difference between the smooth and mid-rough models. Thus, the UHPC-HSC connections with the rough surface remain fully bonded, and are almost equally effective in transferring the load between concrete components. For the smooth and mid-rough models, the de-bonding between UHPC and HSC was accorded at load of 115.4 and 139.5 kN (25.9 and 31.4 kip), respectively.

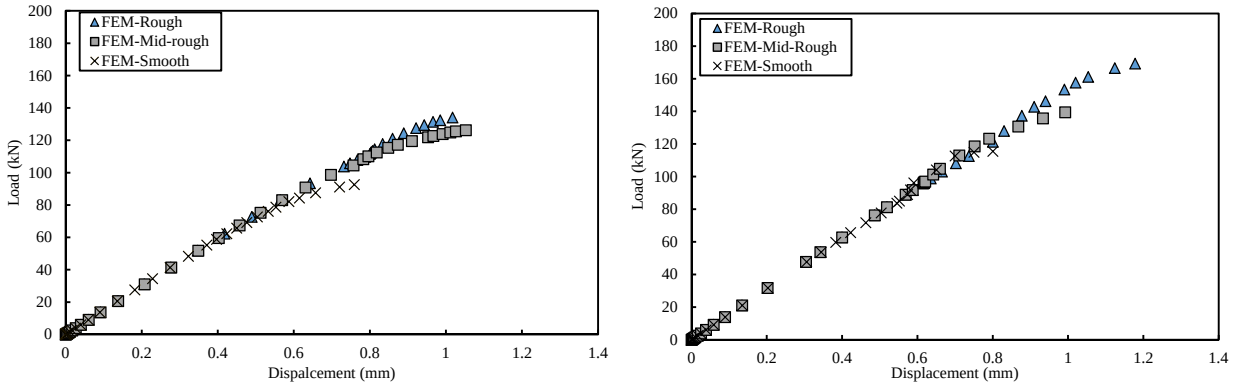

Figure 5. Load-displacement plot with results for different interface models of direct shear specimen using (a) FHWA-UHPC shear key configuration and (b) OPT-UHPC shear key configuration (Note: 1 cm = 0.39 in, 1 N =0.22 lb)

The average maximum load of the FHWA-UHPC design for rough, mid-rough, and smooth surfaces are 134.1, 126.5, and 92.3 kN (30.1, 28.4, and 20.7 kip), receptively, compared to 169.5, 139.2, and 115.2 kN (38.1, 31.3, and 25.9 kip) for the OPT-UHPC design. Thus, the OPT-UHPC design has an ultimate load capacity 26.4, 10.0, and 24.8% larger, even though the cross-sectional areas are approximately equal, 19,677 mm^2 (30.5 in^2) for FHWA-UHPC and 20,161 mm^2 (31.3 in^2) for OPT-UHPC, a difference of about 2.5%. Compared to the FHWA-UHPC, OPT-UHPC increased the maximum load capacity for all different roughness types. This means the OPT-UHPC shear key enhanced the strain distribution between concrete components and as result improved the load transfer. This indicates the load transfer mechanism is substantially influenced by the shear key configuration along with different interface roughness types.

From the analysis in the previous section, it may be concluded that the UHPC shear key is adequate to transfer the load between adjacent concrete components. However, the behavior of the shear key at capacity may also be of interest. Therefore, additional investigations were conducted to determine the failure load and mechanism of the connection. To do so, failure of the UHPC shear keys was defined by the initiation of plastic strain in the joint. For both connections (OPT and FHWA joints) for mid-rough and rough interfaces, failure always began by forming cracks through the HSC components and at the interface in HSC at load failure. For smooth interface both connections, the de-bonding between UHPC and HSC took place. It should be noted that in all models, the FHWA-UHPC shear key were intact, no damage elements while the OPT-UHPC connection that had damage elements at the side of the joint with rough and mid-rough interface models. This indicates that the OPT-UHPC configuration utilizes all the benefit of the UHPC strength and maximizes the transferred load via the OPT-UHPC joint.

To better understand the effect of shear key configuration along with the different interface roughness types on the UHPC-HSC connection capacity for the shear loading case. Within the FE program, the DIC value is calculated by taking the ratio of the actual adhesive stress value at the interface to the maximum value in the normal and tangential directions. It should be noted that each contour is scaled differently to accommodate the wide range in DIC values, but that the average DIC values for FHWA-UHPC shear key side at load of 81.3 kN (18.3 kip) are 0.276, 0.310, and 0.472 for the rough, mid-rough, and smooth surfaces, respectively (see Figure 6(a to d)). For OPT-UHPC shear key, the average DIC values at the same load are 0.331, 0.382, and 0.716 for the rough, mid-rough, and smooth surfaces, respectively (see Figure 6(e to h)). The results indicate that the connection with the smooth surface is closer to reaching capacity than the

connection using the mid-rough and rough surfaces, as might be expected. The high capacity of the mid-rough and rough surfaces can be attributed to a combination of high adhesion and friction due to increased bonding surface and aggregate interlock. Also, the FHWA-UHPC connection with the smooth surface is closer to reaching capacity than the OPT-UHPC connection using the smooth surface, as shown (see Figure 6(d and h)). For mid-rough and rough interface models, the OPT-UHPC shear key showed higher shear strengths than the FHWA-UHPC connection. For both OPT-UHPC and FHWA-UHPC connections, failure always began with cracks in the HSC components. For the FHWA-UHPC connection, the UHPC shear key remained intact, with no cracks in the FHWA-UHPC shear key itself, while the OPT-UHPC connection had cracks in the UHPC at the two sides of the joint using mid-rough and rough interface models.

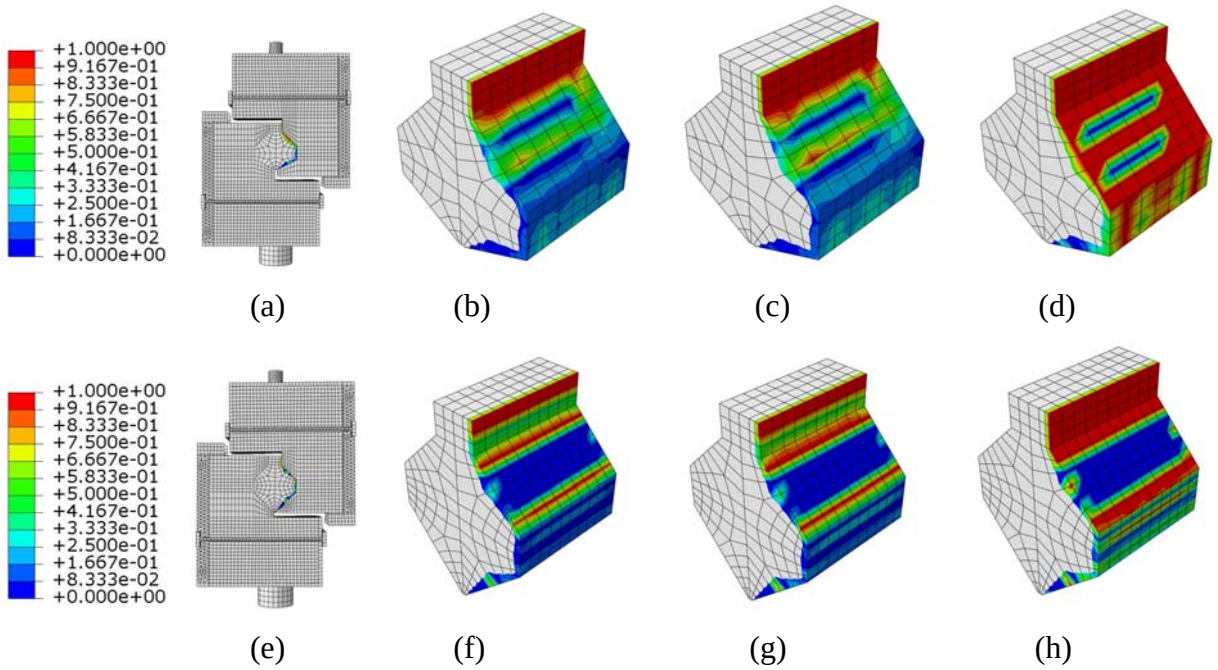

Figure 6. The DIC at interface between UHPC and HSC of (a) FHWA-UHPC connection, for (b) rough, (c) mid-rough, and (d) smooth interfaces along with (e) OPT-UHPC connection, for (f) rough, (g) mid-rough, and (h) smooth interfaces at load of 81.3 kN (18.3 kip)

5 Conclusions

A three-dimensional finite element model was created using Abaqus to evaluate the performance of OPT and FHWA-UHPC shear keys under direct shear load. Three types of surface roughness, rough, mid-rough, and smooth, were adopted for the interface between UHPC and HSC components. The load was applied up to the failure of the specimen to better understanding the stress distribution and failure modes associated with each connection. Based on the results obtained from this research, the following conclusions can be drawn:

1. The OPT-UHPC increased the maximum load capacity for all different roughness types compared to the FHWA-UHPC. This means the OPT-UHPC shear key enhanced the strain distribution between concrete components and, as result, improved the load transfer. This indicates the load transfer mechanism is substantially influenced by the shear key configuration along with different interface roughness types.
2. OPT-UHPC shear key models with the different types of interface roughness between UHPC and HSC components shows better performance in terms of the maximum load

capacity compared to FHWA-UHPC shear key models with the same types of interface roughness.

3. The adhesion has a significant contribution to the bond strength at the interface and suggest that sufficient load transfer could be achieved for UHPC-HSC connections with untreated surfaces, resulting in improved constructability and a reduction in cost.
4. In all models, the FHWA-UHPC shear key elements were damage free while the OPT-UHPC shear key elements showed damage at the side of the joint with rough and mid-rough interface models, indicating that the OPT-UHPC configuration more fully utilizes all the benefit of UHPC strength and maximizes the transferred load via the OPT-UHPC joint.

More studies should be conducted to better understand the OPT-UHPC shear key behavior under traffic and environmental load conditions.

6 References

AASHTO, LRFD (American Association of State Highway and Transportation Officials, Load and Resistance Factor Design). (2012). "Bridge design specifications." *Association of State Highway and Transportation Officials, 6th ed*., Washington, DC.

ABAQUS version 6.12-3 [Computer software]. Providence, RI., Dassault Systèmes Simulia.

Aktan, H., Ahlborn, T. M., Attanayake, U., and Gilbertson, C. G. (2005). "Condition assessment and methods of abatement of prestressed concrete box-beam deterioration—Phase I." *MDOT RC-1470, Michigan Dept. of Transportation,* Lansing, MI.

Chen, L., and Graybeal, B. A. (2010). "Finite element analysis of ultra-high performance concrete: Modeling structural performance of an AASHTO Type II beam and a 2nd generation pi-beam" *FHWA-HRT-11-020, No. PB2011-100864*, Washington, DC.

Chen, L., and Graybeal, B. A. (2011a). "Modeling structural performance of ultrahigh performance concrete I-beams." *Journal of Bridge Engineering, 17(5), 754-764*.

Chen, L., and Graybeal, B. A. (2011b). "Modeling structural performance of second-generation ultrahigh-performance concrete pi-beams." *J. of Bridge Engineering, 17(4), 634-643*.

El-Remaily, A., Tadros, M. K., Yamane, T., and Krause, G. (1996). "Transverse design of adjacent precast prestressed concrete box girder bridges." *PCI J., 41(4), 96–113*.

Grace, N., Ushijima, K., Baah, P., and Bebawy, M. (2012). "Flexural behavior of a carbon fiber–reinforced polymer prestressed decked bulb T-beam bridge system." *Journal of Composites for Construction, 17(4), 497-506.*

Graybeal, B. (2014). Design and Construction of Field-Cast UHPC Connections *(No. FHWA-HRT-14-084).*

Graybeal, B. A. (2006). "Material property characterization of ultra-high performance concrete." *Rep. No. FHWA-HRT-06-103, Federal Highway Administration,* Washington, D.C.

Gulyas, R. J., and Champa, J. T. (1997). "Use of Composite Testing for Evaluating of Keyway Grout for Precast Prestressed Bridge Beams." *ACI materials journal*, 94(3).

Gulyas, R. J., Wirthlin, G. J., & Champa, J. T. (1995). Evaluation of keyway grout test methods for precast concrete bridges. *PCI journal,* 40(1), 44-57.

Hussein, H. H., Sargand, S. M., Al Rikabi, F. T., & Steinberg, E. P. (2017a). Laboratory Evaluation of Ultrahigh-Performance Concrete Shear Key for Prestressed Adjacent Precast Concrete Box Girder Bridges. *Journal of Bridge Engineering,* 04016113.

Hussein, H. H., Sargand, S. M., Al-Jhayyish, A. K., & Khoury, I. (2017b). Contribution of Transverse Tie Bars to Load Transfer in Adjacent Prestressed Box-Girder Bridges with Partial Depth Shear Key. *Journal of Performance of Constructed Facilities, 04016100*.

Hussein, H. H., Walsh, K. K., Sargand, S. M., Al Rikabi, F. T., & Steinberg, E. P. (2017c). Modeling the shear connection in adjacent box-beam bridges with ultrahigh-performance concrete joints. I: Model calibration and validation. *J. of Bridge Eng., 22(8), 04017043*.

Hussein, H. H., Walsh, K. K., Sargand, S. M., and Steinberg, E. P. (2016). "Interfacial Properties of Ultrahigh-Performance Concrete and High-Strength Concrete Bridge Connections." *Journal of Materials in Civil Engineering, 04015208.*

Hussein, H. H., Sargand, S. M., & Steinberg, E. P. (2018a). Shape Optimization of UHPC Shear Keys for Precast, Prestressed, Adjacent Box-Girder Bridges. *Journal of Bridge Engineering, 23(4), 04018009.*

Hussein, H. H., Sargand, S. M., Al Rikabi, F. T., & Steinberg, E. P. (2018b). Experimental validation of optimized ultra-high-performance concrete shear key shape for precast pre-stressed adjacent box girder bridges. *Construction and Building Materials, 190, 178-190*.

Issa, M. A., Ribeiro Do Valle, C. L., Abdalla, H. A., Shahid Islam, P., & Issa, M. A. (2003). Performance of transverse joint grout materials in full-depth precast concrete bridge deck systems. *PCI journal, 48(4), 92-103*.

Lall, J., Alampalli, S., and DiCocco, E. F. (1998). "Performance of fulldepth shear keys in adjacent prestressed box beam bridges." *PCI J., 43(2), 72–79.*

Miller, R., Hlavacs, G. M., Long, T., and Greuel, A. (1999). "Full-scale testing of shear keys for adjacent box girder bridges." *PCI J., 44(6), 80–90.*

Porter, S. D., Logan Julander, J., Halling, M. W., & Barr, P. J. (2011). Shear Testing of Precast Bridge Deck Panel Transverse Connections*. J. of Perf. of Const. Facil., 26(4), 462-468*.

Russell, H. G. (2009). Adjacent precast concrete box beam bridges: Connection details *(Vol. 393). Transportation Research Board*

Russell, H. G. (2011). Adjacent precast concrete box-beam bridges: State of the practice. *PCI journal, 56(1), 75-91.*

Russell, H. G., and Graybeal, B. A. (2013). "Ultra-high performance concrete: a state-of-the-art report for the bridge community." *Rep. No. FHWA-HRT-13-060, Washington, D.C.*

Sargand, S. M., Walsh, K. K., Hussein, H. H., Al Rikabi, F. T., & Steinberg, E. P. (2017). Modeling the shear connection in adjacent box-beam bridges with ultrahigh-performance concrete joints. II: Load transfer mechanism. *Journal of Bridge Engineering, 22(8), 04017044.*

Yuan, J., and Graybeal, B. (2016). "Full-Scale Testing of Shear Key Details for Precast Concrete Box-Beam Bridges." *Journal of Bridge Engineering, 04016043.*